Additive Manufacturing 58 (2022) 102993

Contents lists available at ScienceDirect

Additive Manufacturing

journal homepage: www.elsevier.com/locate/addma

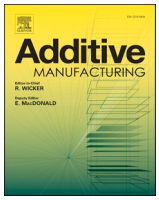

Research paper

A computational design approach for multi-material 4D printing based on interlocking blocks assembly

Kheira Benyahia [a], Hichem Seriket [a], Romaric Prod'hon [a], Samuel Gomes [a], Jean-Claude André [b], H. Jerry Qi [c], Frédéric Demoly [a,*]

[a] ICB UMR 6303 CNRS, Univ. Bourgogne Franche-Comté, UTBM, Belfort, France
[b] LRGP UMR 7274 CNRS, University of Lorraine, Nancy, France
[c] G.W.W. School of Mechanical Engineering, Georgia Institute of Technology, Atlanta, GA 30332, USA

ARTICLE INFO

Keywords:
4D printing
Design for 4D printing
Smart materials
Computational design
Voxel-based modeling
Interlocking blocks

ABSTRACT

4D printing is considered as a disruptive manufacturing technology for creating innovative devices able to evolve in their usage environment. By coupling additive manufacturing (AM) processes and active/passive materials under the effect of an energy stimulation, objects can change properties, shapes, or even functionalities. To achieve a desired shape-change, recent advances in computational design around digital materials require tackling multi-material 4D printing. However, the deposition of active and passive materials in a single run remains difficult due to the different AM techniques required. To overcome this limitation in the context of complex materials distributions, an original approach is to address multi-material 4D printing from the perspective of interlocking blocks assembly. Therefore, the objective of the paper is to propose a computational design approach that converts a multi-material 4D object with a computed digital materials distribution into suitable interlocking blocks. The latter can be printed separately using single material AM and then assembled to achieve the targeted shape change. An implementation of the approach via a dedicated plugin within a computer-aided design environment is presented. A case study is introduced to illustrate the relevance and the applicability of the proposed approach.

1. Introduction

Over the last decades, production strategies, materials development, and manufacturing technologies have greatly influenced design models and approaches to deliver innovative products with new usage modes. These competitive drivers are further emphasized in the context of Industry 4.0 and its main pillars, such as high functionality and high connectivity products and systems, Internet of Things, (soft) robotics, additive manufacturing (AM), and artificial intelligence (AI), to name a few. AM is a relevant manufacturing technology to increase products/parts capabilities in terms of shapes, properties, and functionalities. Since the first 3D printing patent in 1984 [1], AM has received exponential interest from academia and industry, leading to both incremental and disruptive innovations [2]. Among the AM-related innovations [3], 4D printing particularly aims at combining AM and smart materials (SMs) to build shape-, property- or functionality-changing objects under the effect of energy stimulation like heat, pH, moisture, light, electric field, magnetic field, mechanical, etc. [3,4]. Seen as an emerging and interdisciplinary research domain, 4D printing gathers multiple perspectives and interests, ranging from design and engineering [5], mechanical modeling [6,7], manufacturing [8], material science [9,10], chemistry [11], soft robotics [12–16], medicine [17,18], and aerospace [19].

Among the numerous proofs-of-concept proposed in the literature, one can notice research efforts in single-material deposition and multi-material deposition 4D printing [4,20–23]. Although both research directions deserve to be investigated to increase the body of knowledge in 4D printing, it becomes vital to rise this technology in a way to meet industrial applications, especially in terms of mechanical behavior, robustness, reversibility, responsivity, etc. In such a context, multi-material 4D printing offers more freedom in design and engineering to develop active composite structures exhibiting well-balanced soft and structural properties. This research direction leads to novel design approaches and new geometric representation falling under voxel-based modeling and digital materials [24,25]. Indeed, recent efforts have emphasized the need to tackle 4D printing from a design

* Corresponding author.
E-mail address: frederic.demoly@utbm.fr (F. Demoly).

https://doi.org/10.1016/j.addma.2022.102993
Received 21 March 2022; Received in revised form 4 June 2022; Accepted 21 June 2022
Available online 23 June 2022

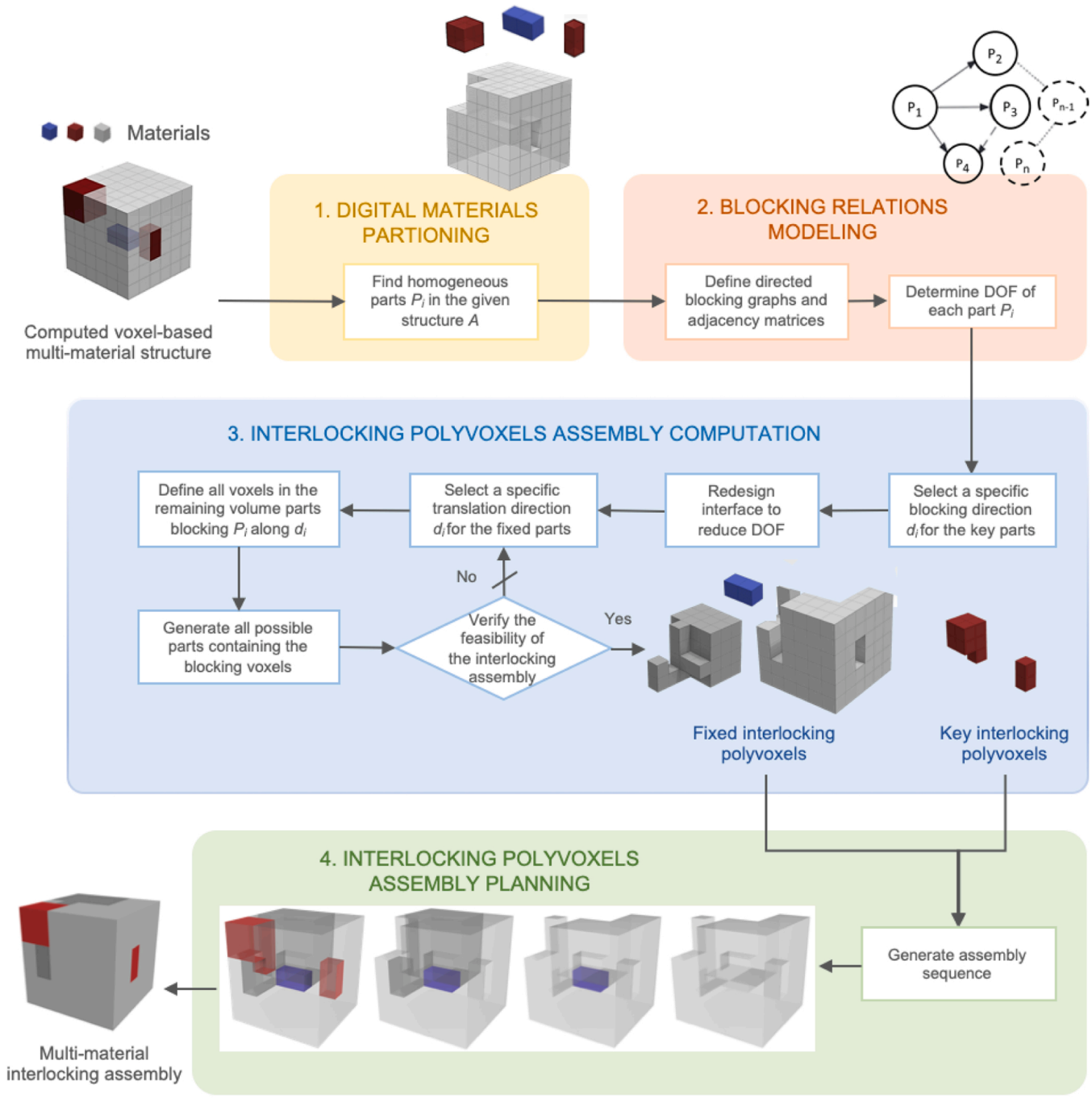

Fig. 1. Flowchart of the computational design for multi-material 4D printing based on interlocking blocks assembly computation.

perspective, introducing the issue of design with/for 4D printing [5,21,26]. The ultimate objective is to allocate the right material (passive and active) at the right place and the right energy stimulus at the right time and place while influencing the part's geometry. Therefore, there is a need for computational support and appropriate geometric representation. In principle, it can be argued that today digital freedom can address AM constraints related to different complexities of form, hierarchy, material printability, and functionality [5,27]. However, there are remaining locks for spatial changes due to other kinds of complexity such as the response of the SMs to an energy stimulation, the

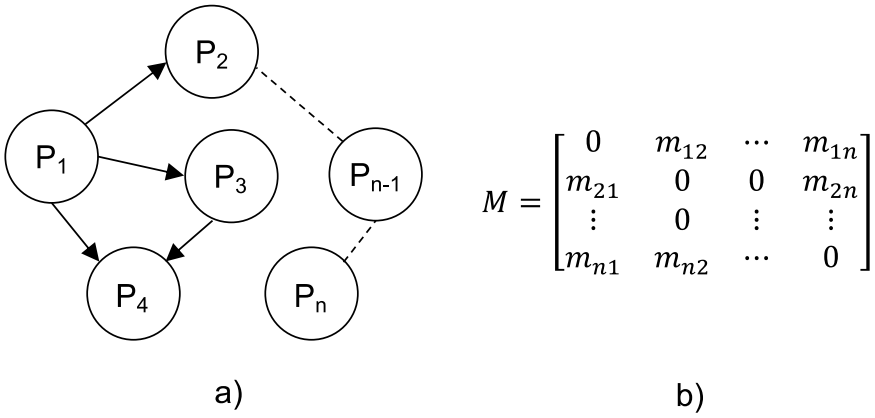

$$M = \begin{bmatrix} 0 & m_{12} & \cdots & m_{1n} \\ m_{21} & 0 & 0 & m_{2n} \\ \vdots & 0 & \vdots & \vdots \\ m_{n1} & m_{n2} & \cdots & 0 \end{bmatrix}$$

Fig. 2. (a) Directed blocking graph $DBG_d = (P, R)$ and (b) its adjacency matrix M according to a specific direction.

location and amplitude of the latter to achieve a desired transformation.

As regards multi-material 4D printing processes, a few AM techniques have been utilized, customized, or combined (hybrid) to suit stimuli-responsive materials printing [5,28–32]. Most of the research investigations concern fused filament fabrication (FFF), direct ink writing (DIW), material jetting (MJ), and digital light processing (DLP). However, recent advances in design computation with digital materials require to develop new multi-material AM strategies [21,26]. Recent works in multi-material 4D printing have illustrated the opportunity to compute materials distributions in three-dimensional structure with the support of AI-based techniques [20,21]. The resulting counter-intuitive distributions are promising to achieve a desired shape-changing behavior while ensuring good mechanical performance. At this stage, most of the numerical results remain difficult to print with the available multi-material AM processes and techniques. An original way of bypassing the limitations of multi-material AM – in terms of AM processes and materials compatibility [33] – is to consider discrete assembly of interlocking blocks with different materials built from multiple AM processes and techniques. A few assembly methods have been investigated in the literature, ranging from bio-inspired interlocking techniques, mechanical interlocking features, and computational interlocking methods [34–44]. Among the approaches ensuring more freedom in terms of material combination, mechanical interlocking with the aid of computational procedures becomes a relevant strategy. It is thus a question of decomposing a 3D model into discrete elements like Lego-like blocks, whether to overcome large parts printing issue or multi-material AM [38,45–50]. Although significant research has been done in this field in terms of computational generation of interlocking 3D assemblies [51–56], a barrier still exists to tackle multi-material 4D printing from an assembly perspective. Here the starting point is a digital materials distribution – obtained from AI-based techniques like evolutionary and genetic algorithms [20,21] – to which a determination of interlocked blocks is sought in the embodiment design stage.

In such a context, the main objective of the paper is to propose a computational design approach for multi-material 4D printing by considering the assembly of discrete 3D printed voxels (or blocks). Addressing such a way enable to build any voxel-based structures which includes either lattice and/or solid units, further falling under both design for 4D printing and design for assembly domains. The proposed approach consists in working with digital materials within a 3D/4D object or structure and determining subsets of polyvoxels (i.e., similar to polycubes in discrete geometry), intended to be printed separately and

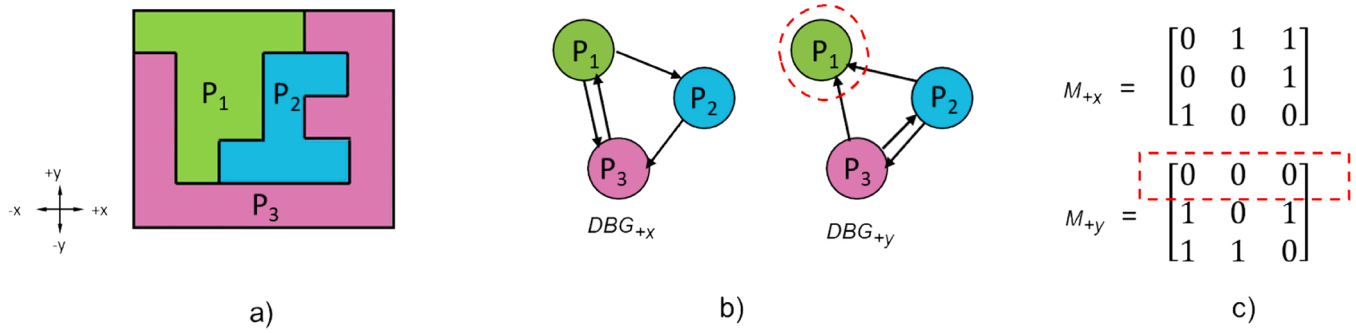

Fig. 3. Example of a (a) 2D assembly of three interlocked parts, with its (b) *DBGs* along the directions $+x$ and $+y$, and (c) the related adjacency matrices. The dashed red circle and rectangle highlight the key part along the $+y$ direction.

then assembled. The scientific originality lies in defining judicious interlocking arrangement of the polyvoxels, ensuring the assembly and the maintenance of the structure, thus, providing more flexible and efficient interlocking methods that are not achieved yet by existing state-of-the-art approaches. For that very reason, we will adopt a voxel-based representation in computer-aided design (CAD) appropriate to multi-material design and 4D printing [21,57–59]. Such a representation provides advantages to (i) describe the overall geometry of the part, (ii) specify the active and inert regions, (iii) allocate properties having a role in transduction, sensing, and actuation, and (iv) distribute materials in the three-dimensional design space [5]. From this, it is then possible to address multi-scale modeling [60–62] with different voxel shapes and structures [63], whether solid, lattice, or even metamaterials [64–69]. The proposal extends prior work on interlocking assemblies [52,55,56,70] by considering as initial input a computed materials distribution in a 4D object via a dedicated CAD plugin [21,26].

The structure of the paper is as follows. Section 2 presents the proposed computational design approach able to analyze digital materials distribution into interlocked blocks. In Section 3, an implementation of the reasoning mechanisms is made via a computational design plugin within a CAD environment, and a case study is introduced to illustrate the relevance of the proposal. Last, discussion and conclusion are provided.

2. Computational design approach for multi-material 4D printing

2.1. Overview

The proposed computational design approach, illustrated in Fig. 1, is composed of four main steps. The first step consists in (i) analyzing the distribution of the digital materials on a voxel basis of a given structure (in the next section, we will use the work of Sossou et al. [21,26] to illustrate complex multi-material structures that are achieved with genetic algorithm), and in (ii) identifying the homogeneous (i.e. same material) set of voxels (also called polyvoxels). The voxels are then categorized according to the properties and/or materials. Afterward, Step 2 introduces the blocking relations modeling. It involves mathematical models to define blocking relations between the identified polyvoxels in Step 1 and determine their degree(s) of freedom (DOF). Step 3 focuses on the interlocking polyvoxels assembly computation and is two-fold: the key (i.e., mobile) interlocking polyvoxels are firstly determined, then fixed interlocking polyvoxels are computed. The last step is dedicated to the interlocking polyvoxels assembly planning. In the following sections, each step is further detailed with an illustrative case.

2.2. Digital materials partitioning (Step 1 of Fig. 1)

This step starts then with the main hypothesis that a pre-computed materials distribution is available through a voxel-based representation. To achieve the desired transformation with a specific stimulation, materials are spatially arranged on a regular voxel grid in the three-dimensional space. At this stage, a partitioning is needed to identify homogeneous parts P_i (voxels or polyvoxels) in the structure (denoted A). This material partitioning represents the first reasoning step to which further analysis will be performed.

2.3. Blocking relations modeling (Step 2 of Fig. 1)

Based on the identified homogeneous parts P_i, the next step consists in modeling blocking relations along the six directions (± x, ± y, ± z). To do so, a directed graph – such as used in [52,55,71,72] – is adopted. Let a directed blocking graph, denoted $DBG_d = (P,R)$, where P is the set of homogeneous parts of the structure A, and R is the set of ordered pairs (arrows) of nodes describing the blocking relations between these parts along the direction d (± x, ± y, ± z). Then, according to this modeling scheme, an ordered pair between P_1 and P_2 means that P_1 is blocked by P_2 along a direction d (see Fig. 2a). The resulting *DBGs* are then converted into adjacency matrices, denoted M, for computation purposes, as illustrated in Fig. 2b. An adjacency matrix M is a square matrix, where entries can be defined as follows (Eq. 1):

$$M = \left[m_{ij}\right]_{i,j \quad \in \mathbb{N}^* \times \mathbb{N}^*} \tag{1}$$

with.

$\left\{ \begin{matrix} m_{ij} = 1 \\ m_{ij} = 0 \end{matrix} \right\}$ if P_i is blocked by P_j in a given direction.

if there is no blocking relation between P_i and P_i in a given direction.

Parts (voxels or polyvoxels) are assumed to be assembled through one single translational motion. In such a context, parts exhibiting mobility will be considered as “key” parts (i.e., parts ensuring the mechanical fastening of the assembly and eventually requiring an adhesive bonding operation). To illustrate the principle of modeling the blocking relations of the parts in an assembly, Fig. 3 introduces a two-dimensional assembly composed of three interlocked parts, namely P_1, P_2, and P_3, to which DBG on $+x$ and $+y$ directions (denoted DBG_{+x} and DBG_{+y}) and related adjacency matrices (denoted M_{+x} and M_{+y}) have been defined.

An assembly A is deemed to be interlocked, if each of its single parts and subassemblies are blocked along all directions once positioned, except the key(s) part(s) that has(have) the freedom of moving on one imposed direction (see Fig. 3a,b). In order to determine the DOF of the parts P in the assembly A, the computation of blocking relations along all translation directions is required with the support of related adjacency matrices. For instance, if all the entries m_{ij} in a row i of an adjacency matrix M_d are equal to 0, then it indicates that the part P_i is mobile along the direction d (see P_1 in Fig. 3a,c) and gains in this manner 1 DOF.

2.4. Interlocking parts assembly computation (Step 3 of Fig. 1)

Built on this, a computation step is needed to determine interlocking parts (whether voxels or polyvoxels) to build the multi-material 3D/4D structure. The proposed Algorithm 1 aims to define judicious interlocking arrangement of homogenous polyvoxels intended to be printed separately using different AM processes and materials and then assembled. It exhibits two reasoning layers: (i) first, parts with DOF > 1 are redesigned to reduce their DOF and set as key parts subsequently (see Algorithm 1, lines 15–25); (ii) then, parts with DOF $= 0$ (i.e., embedded parts) are liberated to enable their assembly, through a generation of additional interlocking parts from the embodying volume. The computational iteration of these interlocking parts takes into account the aforementioned key parts and their insertion directions in the assembly (see Algorithm 1, lines 27–43). Parts with DOF$= 1$ are automatically considered as key parts. The following will lay out the algorithm objectives with more details.

Algorithm 1. Interlocking parts assembly computation.

Input: Set of homogeneous parts of the structure (see Fig. 4a)
Output: Set of interlocking parts for multi-material assembly

Set P the list of all parts
Set MP the list of mobile parts
Set Lvm the list of all voxels forming the mobile parts
Set FP the list of fixed parts
Set Lrv the list of voxels in the remaining volume
Set DOF_{MP} list of DOF of mobile parts
Set KP list of key parts
Use the directed graphs and adjacency matrices to deduce DOF of each part MP_i in MP.
foreach part MP_i in MP **do**
    Move MP_i toward all directions
        if move MP_i in d_i = = not null **then**
            $\{DOF_{MPi} + 1$ in $d_i\}$
            Deduce DOF of MP_i
        end
    if DOF_{MPi} >1, **then** Define key parts
        Add MP_i to KP as a key part
        Decrease DOF_{MPi} to 1
        Keep MP_i mobile toward one and only one random direction d_i, and block it
        toward the other directions (Condition 1)
        Set Lvn_1 the list of all voxels from Lrv neighboring MP_i (see Fig. 4b)
        foreach voxel Vn_{1i} from Lvn_1 that fulfills (Condition 1) **do**
            Pick a random voxel $Vn_{1'}$ (see Figs. 4c,d)
            Add $Vn_{1'i}$ to MP_i (Figs. 4c,d)
            Update MP_i, P, MP, KP, Lvm and Lrv
            Rank the assembly of MP_i as a key part
        end
    else if $DOF_{MPi} = 0$ **then**
        Set P_{DOF0} list of parts with DOF = 0
        Increase DOF of parts in P_{DOF0}
        foreach part P_i in P_{DOF0} **do**
            Add P_i to FP
            Set d_i a random direction as the direction of the insertion of P_i
            Set Lvn_2 the list of all voxels Vn_{2i} from Lrv blocking P_i along d_i (Fig. 4e)
            Generate possible parts containing Vn_{2i}. The generated parts must have 1
            DOF before the insertion of the key part, and DOF = 0 once the key parts
            are inserted (Condition 2) (see Figs. 4f,g)
            if there are possible solutions fulfilling (Condition 2) **then**
                Set Lpg the list of all the generated parts
                Pick a random part Lpg_i from Lpg
                Add Lpg_i to FP
                Update MP_i, P, FP, MP, Lvm and Lrv
            else if there are no possible solutions fulfilling (Condition 2) **then**
                Backtrack and change direction d_i
            end
        end
    end
end
Return interlocking parts

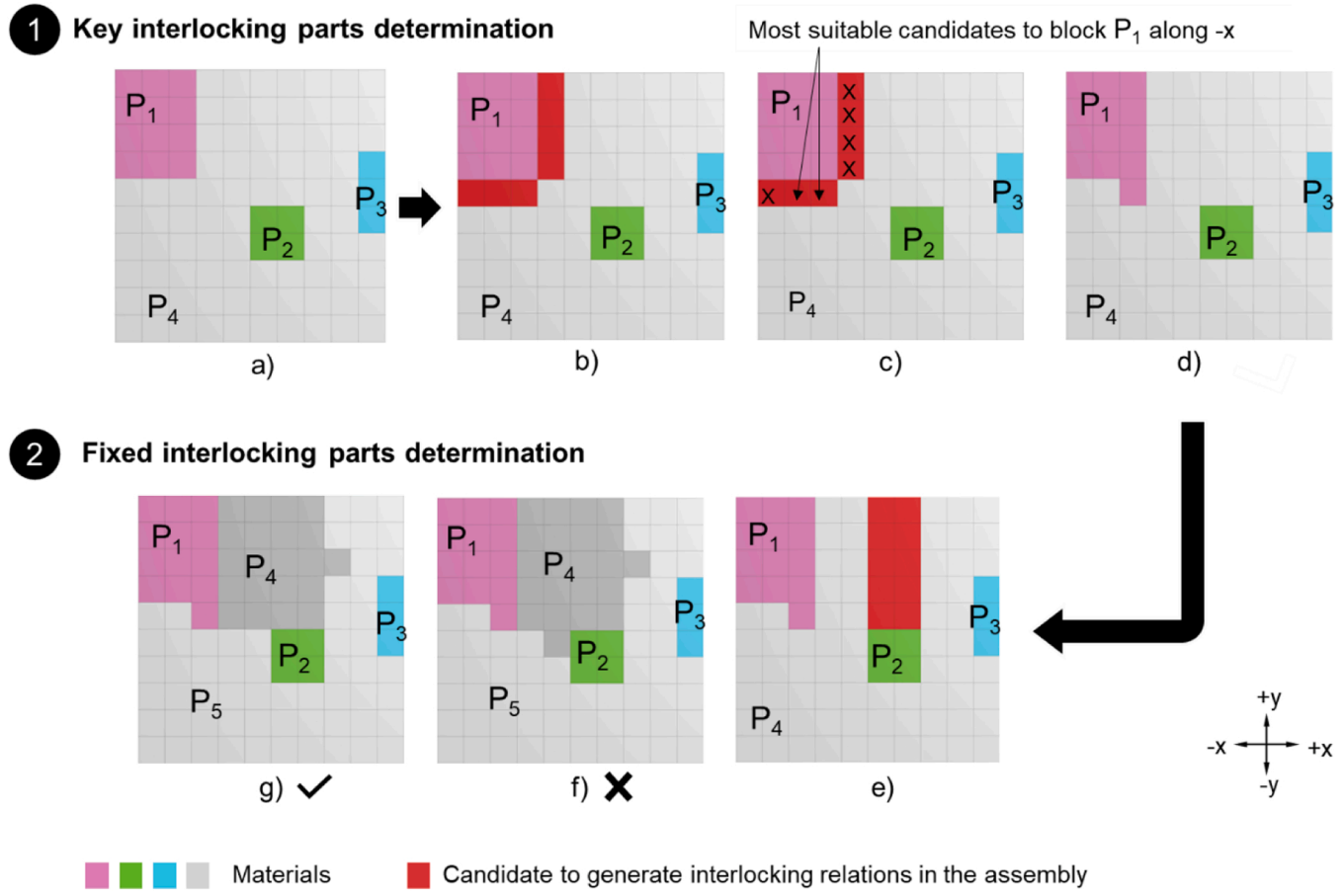

Fig. 4. Insight of the computational approach to generate a multi-material interlocking assembly leaning on DBGs and adjacency matrices: (a) the input structure is of 10 × 10 voxel-based representation of a random digital material distribution, (b) neighboring voxels of mobile part highlighted in red, (c) selection of the most suitable candidate to generate the key part, (d) key part redesign, (e) voxels blocking P_2 toward +y direction in red, (f) P_4 cannot be inserted into the assembly (not suitable as a solution), (g) generation of a suitable interlocking part.

By processing the above-described algorithm, iterative computations might be time-consuming due to the complexity of the imposed multi-material 3D/4D structure. To overcome this potential computational limitation, slight modifications in the digital material distribution are allowed while maintaining the desired shape-changing or property-changing behavior. Thus, to ensure the interlocking and the assemblability of the generated parts, the following conditions must be considered:

1) Slight modifications in the digital material distribution when required;
2) One and only one translation direction is allowed to insert each part in the assembly;
3) The sub-assembly $\{P_i, A\}$ is interlocking with the part P_{i-1}. In other words, P_{i-1} blocks the sub-assembly $\{P_i, A_i\}$ once assembled and so on until the key part(s) is(are) lastly inserted to secure the entire assembly;
4) P_{i-1} can be disassembled from $\{P_{i-1}, P_i, A\}$ along one translation direction (key part(s) is(are) the first to disassemble).

To illustrate this step, a two-dimensional assembly composed of four homogeneous parts is introduced in Fig. 4. It shows a randomly computed distribution of materials through a voxel-based representation of the object. In this illustrative case, P_1, P_2, P_3, and P_4 are respectively composed of a specific material (or bear a specific property). First the key parts are generated by reasoning on the related *DBGs* and adjacency matrices, then the fixed interlocking parts determination is addressed.

2.4.1. Key interlocking parts determination

Since the key parts are the only mobile parts in the assembly, we will set them among parts with a DOF ≥ 1, as illustrated with P_1 and P_3 in Fig. 4a. As for parts exhibiting a DOF > 1, i.e., allowing more than one translation motion as P_1 in Fig. 4a, a slight modification has to be made in the initial dissection in order to ensure its interlocking. Suppose that the key part (P_1 in the illustrate case), is movable along *-x* and *+y* directions and the objective is to block its motion in the *-x* direction. To do so, all the neighboring voxels to the candidate key part are selected (i.e., they share one side with the key part), then a random candidate voxel fulfilling the blocking condition is picked. Once the candidate voxels are identified and selected, they are added to the key parts (as illustrated in Fig. 4b,c,d). In such a way, the single translation of the key parts is ensured.

2.4.2. Fixed interlocking parts determination

The illustrative case in Fig. 4a shows one part (P_2) embedded in a larger one (P_4). In order to solve this dilemma, the following process can be applied as follows:

1) Pick a random direction d_i to insert the desired part (for instance in Fig. 4, +y direction is selected to insert P_2);
2) Select all the voxels blocking the motion of the desired part along d_i as candidate voxels of interlocking part generation (see Fig. 4e);
3) Generate all possible parts containing the aforementioned candidate voxels (see Fig. 4f,g for examples of generated part possibilities);
4) Pick a proper part among the generated interlocking parts. Considering that the key parts blocks $\{P_i, A\}$ once assembled, the generated

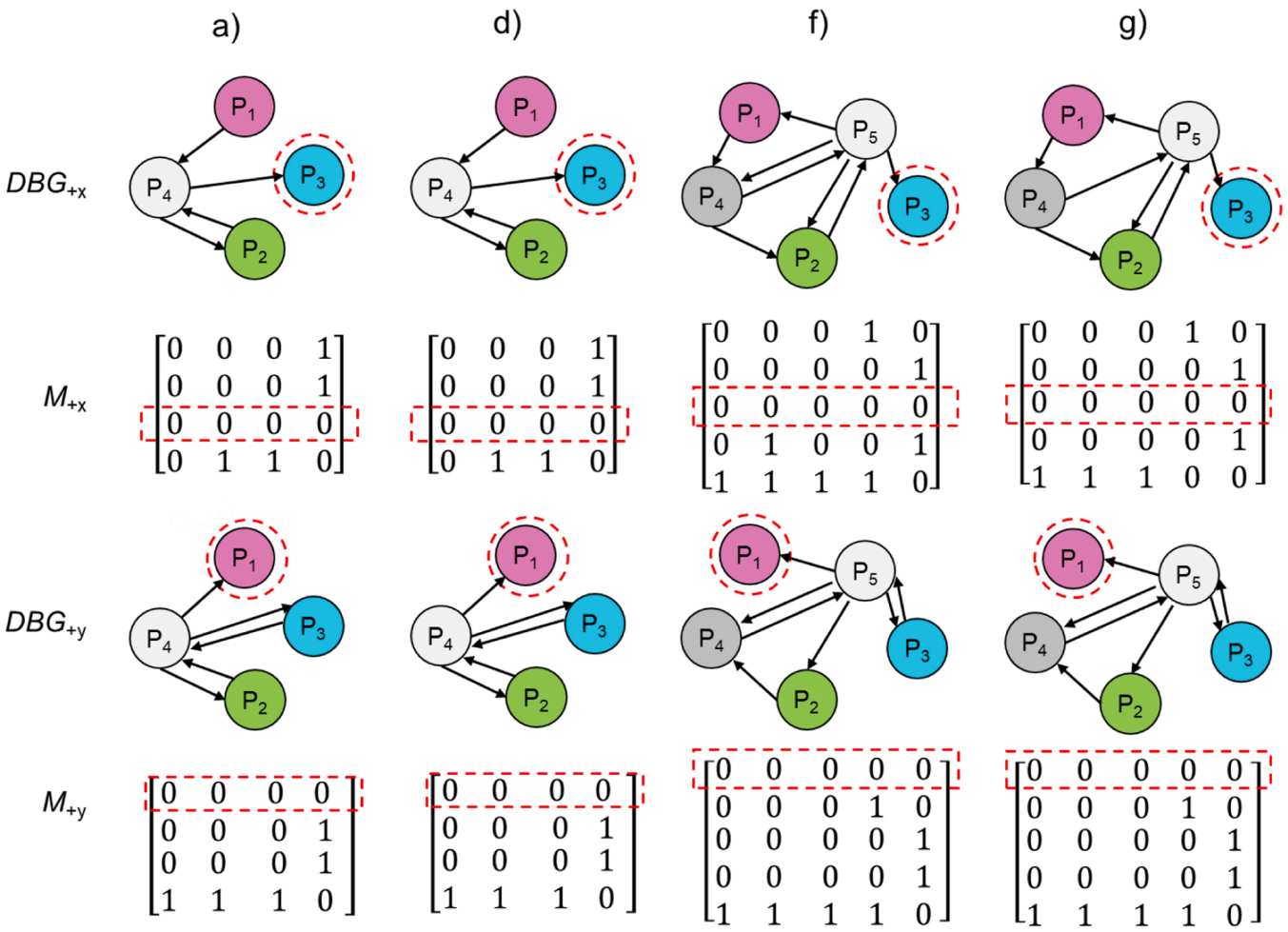

Fig. 5. DBGs and M on +x and +y directions related to cases a, d, f, and g of Fig. 4. The dashed red circle in the DBGs and rectangle in matrices refer to key parts in the specific direction.

part P_4 in Fig. 4g needs to be inserted in the assembly *A* along one single translation direction ($+x$) and blocked along all direction once the key piece(s) is(are) assembled;

If there are no possible interlocking parts along the chosen direction, then we should backtrack and restart the above actions with a different direction.

2.5. *Interlocking parts assembly planning (Step 4 of Fig. 1)*

Following the computation of the interlocking parts, the last step addresses the assembly sequence planning. This critical step aims at determining the assembly order of the generated interlocking parts to build the multi-material 3D/4D structure. To do so, the blocking relations information are used as well as the reasoning layers of Algorithm 1. Once the interlocking parts are generated, they will be ranked according to their generation order. Afterward, we will reverse the order of interlocking parts computation to obtain the assembly sequence; in other words, the first generated parts (key parts) are the last to be inserted to the assembly, which is logically fitting since the key parts are the only mobile parts and block the remaining parts in the assembly. For example, if we follow the interlocking parts computation order in Fig. 4g, P_3, as key part, was firstly generated as it had only one DOF, then the creation of the second key part P_1 followed. Later, the extraction of P_4 took place to enable the insertion of P_2 into the remaining volume P_5. Therefore, the assembly sequence of the case g in Fig. 4 is as follows: {P_5, P_2, P_4, P_1, P_3}.

Fig. 6 on the other hand, illustrates a 3D model of interlocking blocks assembly iteration and their assembly sequence. Starting from a voxelized multi-material/properties cube with an edge length of six voxels, the interlocking parts were generated successively. Thereafter, the assembly sequence has been determined to finally reach a multi-material/properties interlocking assembly.

3. Results and discussion

The proposed approach is dedicated to assembling 3D/4D structures with a pre-computed materials distribution addressed through a voxel-based representation. To do so, we use the work of Sossou et al. [21, 26] to compute a preliminary materials distribution in the structure with the aid of genetic algorithms to fulfil a desired shape-changing behavior. Then, our computational design approach aims to determine the interlocking blocks to be 3D printed and assembled, therefore leading to a complex 3D/4D object achieving the desired shape change. In this section, the relevance and applicability of the proposed approach are illustrated, by introducing a case study covering 4D voxelized structures with computed material distributions.

3.1. *Materials and fabrication*

The proposed case study is a beam with a specific shape change. The design of the beam is described with a voxel-based representation for materials distribution a multi-shaped digital distribution of an inert material and an active material via VoxSmart add-on, a Grasshopper

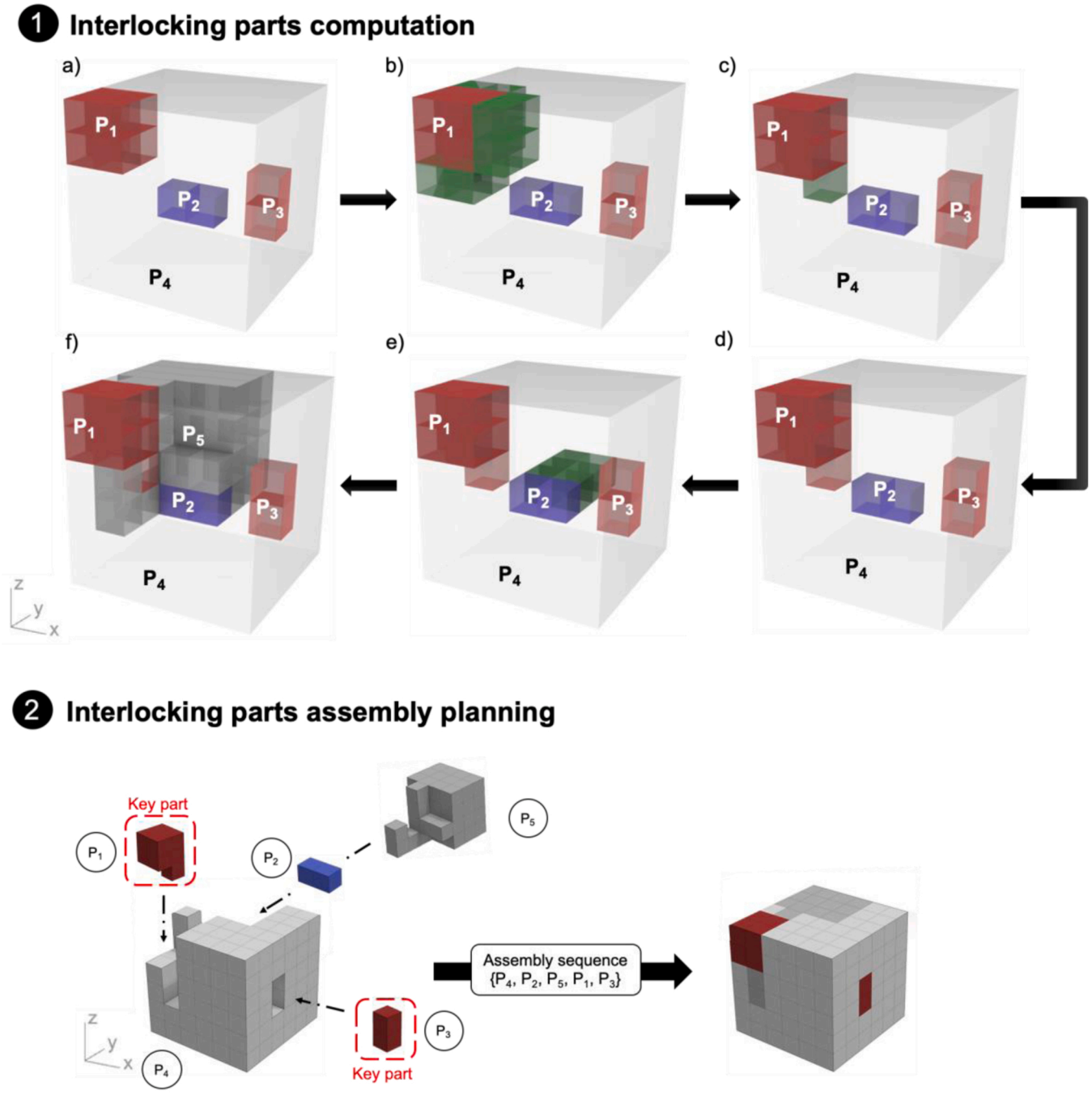

Fig. 6. Illustrative case showing 6 × 6 × 6 voxelized multi-material cube (1) the interlocking parts computation: (a) input structure, each voxel color refers to a type of material/property, (b) to (d) key part generation, (e) and (f) refer to fixed interlocking parts generation. (2) Assembly sequence planning of the generated interlocking parts: (a) insertion direction of each interlocking part, (b) the assembly order, (c) a multi-material interlocking assembly.

plugin in Rhinoceros3D environment [21–26] (Fig. 7a,b). The sample is 18 × 18 × 126 mm^3, containing 1512 voxels (3^3 mm^3 per each voxel). To design the shape-changing structure, we used a soft material (Agilus30, Stratasys, USA, tensile strength~2,4 MPa) printed with a Objet260 Connex3 machine (Stratasys Ltd., USA) as passive material. The machine leverages a MJ technique called PolyJet. A temperature-sensitive hydrogel is used as active material. The material has been printed by using DIW with a Hydra 16 A machine (Hyrel3D, Norcross, USA) and a stepper controlled EMO-25 extruder (Hyrel3D, Norcross, USA). To ensure the shaping of the hydrogel blocks, SUP706B™ (Stratasys, Rheinmüster, Germany) molds were built with the Objet260 Connex3 machine because of the ability of the material to be removed manually without damaging the hydrogel. This thermo-responsive hydrogel has been adopted due to its ease of formulation and extrusion with DIW, its non-toxicity and biocompatibility. This hydrogel shrinks when exposed to heat. The exhibited shape change is an isotropic shrinkage and there is lower threshold by which the dimension's change begins (usually referred to as lower critical solution temperature – LCST). Away from the critical temperature, the change stops, as the material reaches equilibrium collapsed state. The hydrogel was prepared according to the work of Lai et al. [73]. It is composed Alginate (Alg) and Methylcellulose (MC). First, Alg powder is added into a Calcium Chloride solution (0.075% w/v) to obtain a homogeneous 3% (w/v) Alg hydrogel. The solution is then heated to about 80 °C and MC powder with 9% (w/v) is added to obtain Alg/MC hydrogel. The chemical mixture is magnetically stirred until the

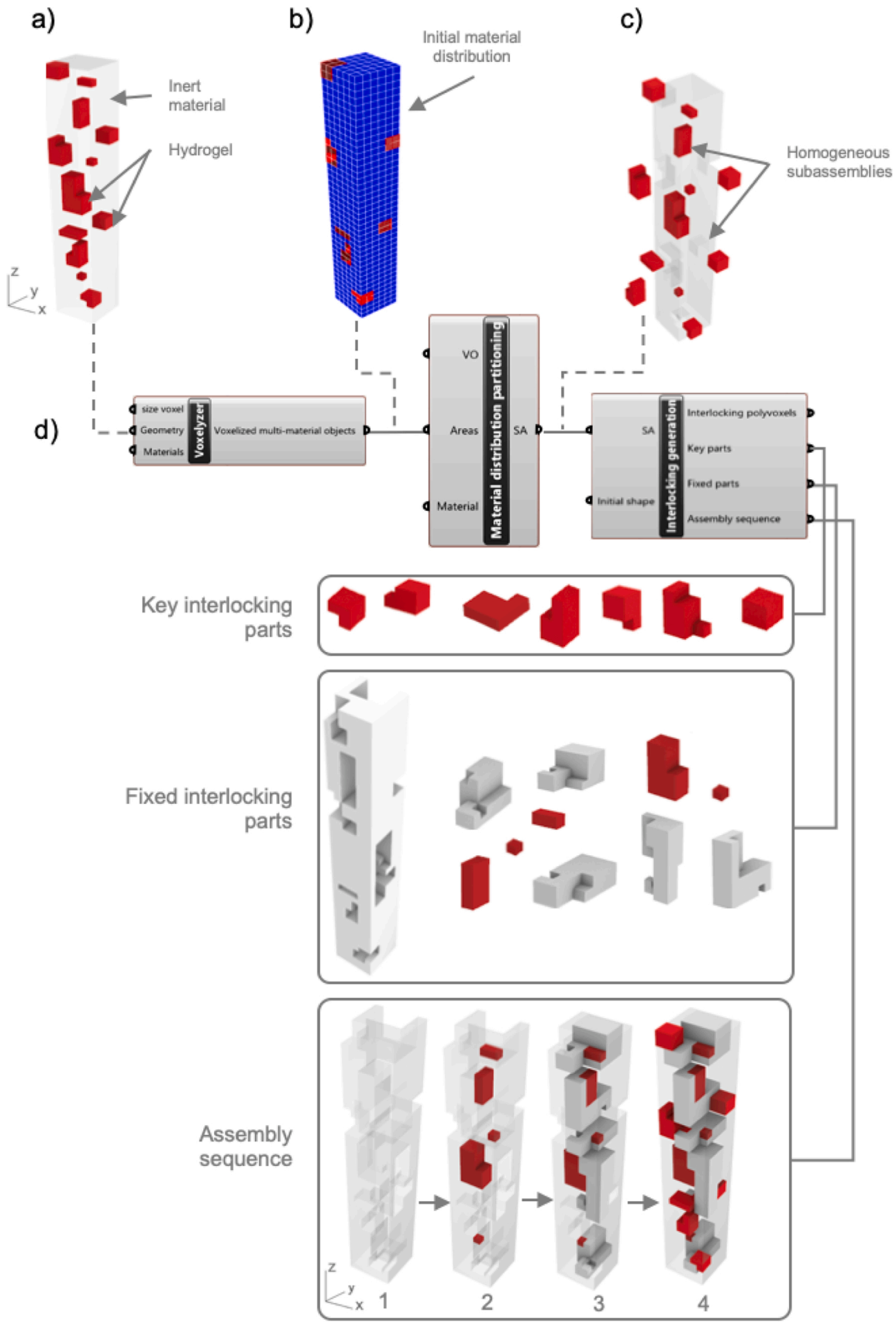

Fig. 7. Illustration of a 18 × 18×126 mm^3 multi-material structure interlocking assembly generation steps: (a) initial structure, (b) initial distribution, (c) homogeneous subassemblies after material distribution partitioning, and (d) design program flow within the VoxSmart add-on in Grasshopper for the interlocking computation.

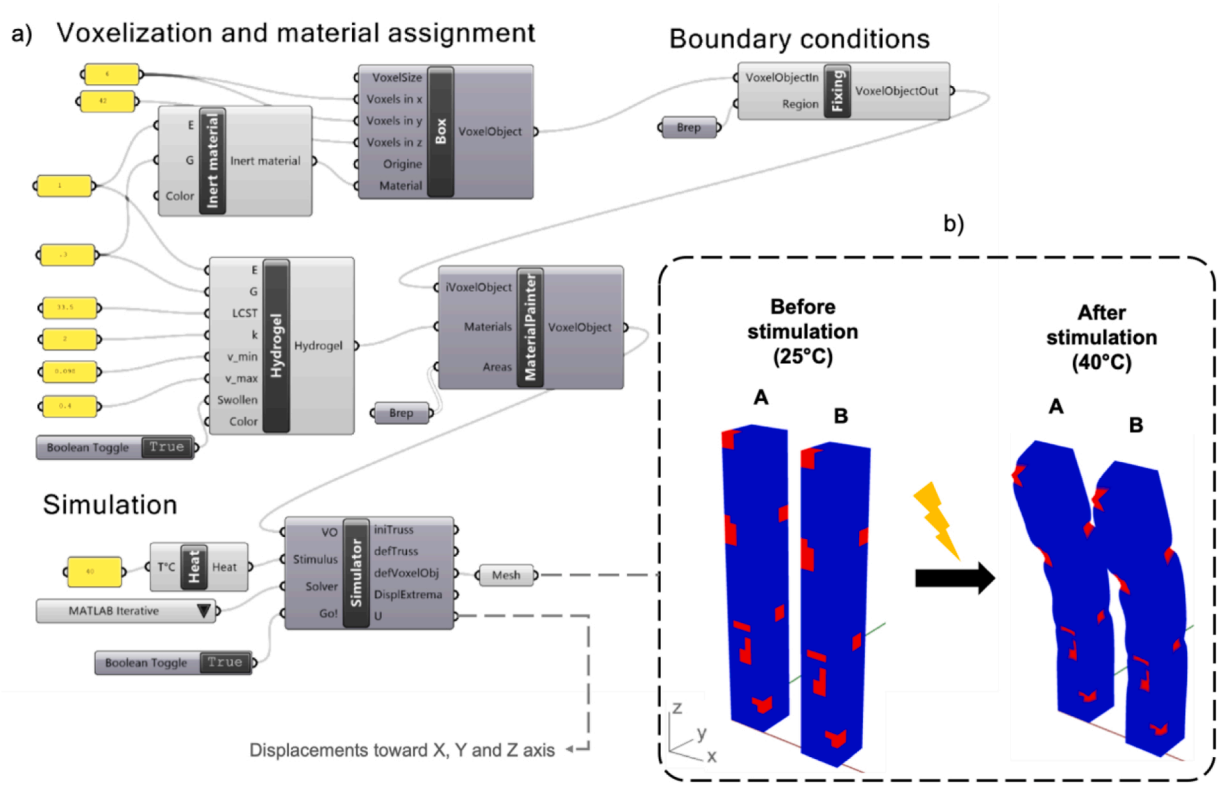

Fig. 8. Simulation of the original distribution deformation (A) and the interlocked distribution (B): (a) VoxSmart program flow for voxelization, materials assignment (inert material: Agilus30; active material: hydrogel), and SM simulation, (b) A and B distributions before thermal stimulation (at 25 °C) and after stimulation (at 40 °C).

dissolution of MC powder to finally obtain a printable Alg3/MC9 hydrogel (viscosity ~5.10^3 Pa.s).

3.2. *Interlocking assembly generation results*

In this section, an implementation of the computational approach via new developed VoxSmart components within Rhinoceros3D/Grasshopper environment is presented. It consists in three dedicated components: (i) the "Voxelyzer" component has been developed to obtain a voxel-based representation of the materials distribution, (ii) the "Material distribution partitioning" component to section the given structure into homogeneous parts, and (iii) the "Interlocking generation" component to generate a set of key parts and fixed parts with a proper assembly sequence. There is more than one possible solution that can be generated by the interlocking blocks assembly algorithm, since the directions of insertions are randomly chosen in each iteration, as well as the blocking voxels candidates. Here one possible interlocking assembly set is suggested to build the multi-material 4D structure. Fig. 7 illustrates the case study results in terms of digital materials distribution partitioning, interlocking parts generation, and assembly sequence planning. Minor changes has been made in the digital materials distribution to ensure both the interlocking and assemblability of the blocks.

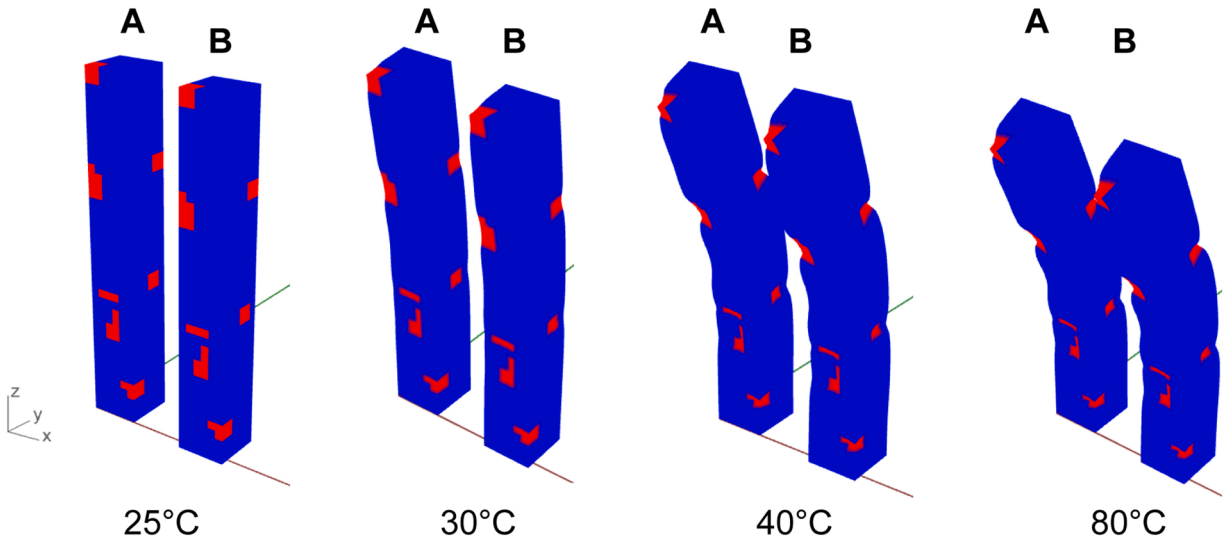

Fig. 9. Numerical simulation with VoxSmart plugin of the initial distribution (A) and adjusted distribution (B) at 25 °C, 30 °C, 40 °C, and 80 °C.

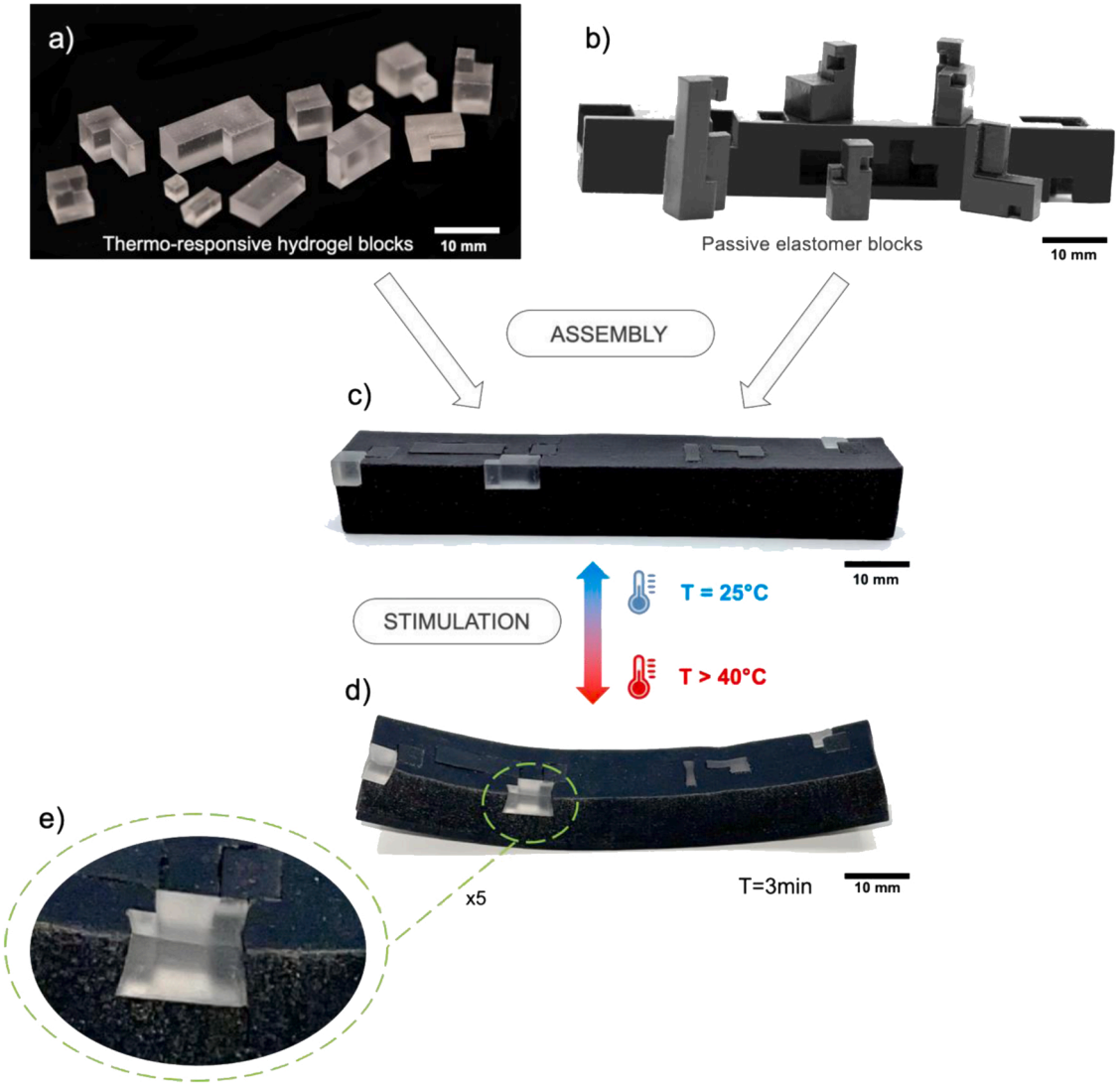

Fig. 10. Multi-material 4D printing via interlocking blocks: (a) thermo-responsive hydrogel blocks printed with DIW technique, (b) Agilus30 blocks printed with MJ (PolyJet technique), (c) manual assembly of the interlocking blocks by following the assembly sequence generated by the developed VoxSmart component, (d) deformed structure after stimulation at 40 °C in water, (e) interlocking assembly deformation zooming in (Focus x5).

3.3. Simulation

As mentioned in Section 2.4, the digital materials distribution is considered as an imposed input, which may lead to complications at the interlocking computation step. Slight modifications of the digital materials distribution can then be allowed when necessary in order to overcome this limitation. The purpose of the simulation phase is to investigate the consequences of the changes regarding the physical behavior of the structure. We target a minor shape-changing difference between the original distribution and the adjusted one once stimulated, while maintaining the physical properties. Figs. 8 and 10 highlight respectively the simulation of the distributions and the change calculation in physical deformations at multiple temperatures. The simulation of the considered case study was carried out using VoxSmart add-on [21,26].

Once the simulation done, the designer will be able to access to detailed information about voxels displacements along *x*-, *y*-, and *z*-axis, via the simulator component (of the VoxSmart add-on) output *U* (i.e., the list of values showing all the DOFs in terms of displacements and rotations of the underlying truss's nodes) as shown in Fig. 8a. In order to compare both distributions in terms of physical behavior the computed displacements are used to measure the distance between the position of each voxel v_i in the original digital materials distribution and its position (v_i') in the adjusted one. To do so, vectors moduli are calculated using the following Eq. (2).

$$\| \overrightarrow{v_i' v_i} \| = \sqrt{(U_{x_{adjusted}} - U_{x_{original}})^2 + (U_{y_{adjusted}} - U_{y_{original}})^2 + (U_{z_{adjusted}} - U_{z_{original}})^2} \quad (2)$$

Where:

$$v_i = \left(U_{xi_{original}}, U_{yi_{original}}, U_{zi_{original}}\right) \quad \text{and} \quad v_i' = \left(U_{xi_{adjusted}}, U_{yi_{adjusted}}, U_{zi_{adjusted}}\right)$$

are the voxel displacements vectors in the original and adjusted distribution respectively.

Table 1
Calculation of the maximum and average distances between voxels' positions in the initial distribution (A) and adjusted one (B) at 25 °C, 30 °C, 40 °C, and 80 °C.

	25 °C	30 °C	40 °C	80 °C
Maximum Distance (10^{-2} mm ± 0.0001)	0	07.74	24.22	24.61
Average Distance (10^{-2} mm ± 0.0001)	0	01.79	05.58	05.68

Taking into account VoxSmart simulation and distances measurement results, we demonstrate in Fig. 9 and Table 1 that the difference in terms of deformation variation between both distributions is slightly different, or even non-existent, regarding displacements along $\pm x$, $\pm y$ and $\pm z$. The narrow modification that has been applied to the digital material distribution in order to generate the interlocking assembly, has not offended the physical properties of the original 4D structure. Therefore, the relevance and the applicability of the proposed approach is demonstrated.

Table 1 provides the maximum and the average distances between a voxel's position in the original materials distribution (A) and its positions in the adjusted one (B). For instance, the largest difference in displacements of a voxel between (A) and (B) at 40 °C, was equal to 0.2422 mm which is fairly negligible. The physical shape change of the case study is illustrated in Fig. 10 where the printed interlocking active and passive blocks (see Fig. 10a.b) are laid out before the manual assembly, after the assembly and after the stimulation. This figure shows a shape change as expected in the design and simulation stages. The change is achieved when the multi-material structure is exposed during 3 min in water at 40 °C. The shape recovery is achieved when water is progressively cooled down to room temperature after 5 min. The shape fixity (i.e. the property of a material to stay at a specific shape once stimulated) is made possible when the object is constantly stimulated.

3.4. Discussion

The proposed research work has particular limitations that can open up captivating directions for future studies. First, to ensure better structural performances of the structure, an complimentary algorithm to generate a multi-scale interlocking polyvoxels will be developed. This strategy will also allow the authors to better control the multi-material distribution interlocking when adjustment is required, so the impact on the physical properties of the structure can be further minimized. It would be also significant to optimize another essential aspect not yet covered in the proposed research work, i.e., the consideration of geometric deviation related to AM processes/techniques capabilities. Modifications in polyvoxels geometries can be caused by AM inaccuracies, that in the context of multiple parts assembly can be magnified, therefore leading to assemblability issues. As such, handling the geometric deviation to overcome the potential limitation, would be an exciting future research problem. This point can also be addressed and solved by using microfabrication technologies like two-photon polymerization.

From a simulation point of view, we adopted Euler-Bernoulli beam theory (as successfully addressed in [21,26]) to simulate the behavior of the materials in the structure where voxel materials are considered as tied. This hypothesis is usually applied in the modeling of active composites (see [20,22,26]). In this paper, interlocking blocks are assumed to follow the same modeling scheme. However, it would be more realistic to integrate the mechanical behavior at the interfaces of the interlocking blocks. Extensive research should cover this avenue to predict the functional fatigue of the interlocking blocks assembly under the effect of multiple cycles of stimulation.

Future work will also be focused on the improvement of the computational procedure to determine interlocking blocks. The use of AI-based techniques may be relevant to solve such combinatorial and time-consuming optimization problem. Further work will investigate the combination of deep reinforced learning and 3D convolutional neural networks. The latter, which leverage spatiotemporal information, are suitable to classify materials distribution and/or interlocking blocks through voxel-based simulation or finite element models. It is also expected to consider other conditions for the interlocking polyvoxels assembly computation such as minimizing printing support, minimizing the variety of polyvoxels depending on the voxels number (i.e., using standard polyvoxels). Last, additional effort will be dedicated to the development of a robotic platform to which polyvoxels can be handling and assembled at various scales.

4. Conclusion

This research work highlights a computational design approach for multi-material 4D printing. By considering a given digital materials distribution fulfilling a desired shape-changing behavior, the approach aims to generate interlocking blocks intended to be printed separately then assembled to build the multi-material 4D structure. On one hand, our computational design enables the creation of an interlocking assembly automatically, rather than its creation by expensive assembly design methods. On the other hand, its generality and efficiency allow to explore new types of complex assemblies that are impossible to be printed via a unique AM technique in a single run, such as combining solid voxels/lattices or metals/polymers in the same assembly. Thus, it enables the integration of dissimilar materials in 4D printed structures such as for instance materials ensuring internal and local stimulation. The illustrative case study, exhibiting a specific shape-changing behavior, has shown the added value of the proposal in terms of computation and realization. The work done opens the door toward promising and innovative applications in multiple domains such as automotive, soft robotics, spatial structures, medical technologies to name a few.

Funding

Funding provided by the French 'Investissements d'Avenir' program, the EIPHI Graduate School (contract ANR-17-EURE-0002).

CRediT authorship contribution statement

Kheira Benyahia: Writing – original draft, Software, Methodology, Conceptualization. **Hichem Seriket:** Software, Conceptualization. Romaric Prod'hon: Software, Conceptualization. **Samuel Gomes:** Supervision. **Jean-Claude André:** Writing – review & editing. **H. Jerry Qi:** Writing – review & editing. **Frédéric Demoly:** Writing – review & editing, Writing – original draft, Supervision, Methodology Funding acquisition, Conceptualization.

Declaration of Competing Interest

The authors declare that they have no known competing financial interests or personal relationships that could have appeared to influence the work reported in this paper.

Data Availability

No data was used for the research described in the article.

Acknowledgements

The authors would like to thank the reviewers for their feedback and comments. This research work has been supported by the French 'Investissements d'Avenir' program, the EIPHI Graduate School (contract ANR-17-EURE-0002), the S.mart academic society and Bourgogne Franche-Comté Region.

References

[1] J.C. André, A. Le Méhauté, O. De Witte, Dispositif pour réaliser un modèle de pièce industrielle, French Patent n° 84 11 241, 16.07.1984, 1984.
[2] F. Demoly, J.C. André, Research strategy in 4D printing: disruptive vs incremental? J. Integr. Des. Process Sci. 24 (2020) 53–73, https://doi.org/10.3233/JID200020.
[3] J.C. André, From additive manufacturing to 3D/4D printing. Breakthrough innovations: programmable material, 4D printing and Bio-printing, ISTE-Wiley, London, UK, 2017.
[4] S. Dimassi, F. Demoly, C. Cruz, H.J. Qi, K.Y. Kim, J.C. André, S. Gomes, An ontology-based framework to formalize and represent 4D printing knowledge in

design, Comput. Ind. 126 (2021), 103374, https://doi.org/10.1016/j.compind.2020.103374.
[5] F. Demoly, M.L. Dunn, K.L. Wood, H.J. Qi, J.C. André, The status, barriers, challenges, and future in design for 4D printing, Mater. Des. 212 (2021), 110193, https://doi.org/10.1016/j.matdes.2021.110193.
[6] S.M. Montgomery, X. Kuang, C.D. Armstrong, H.J. Qi, Recent advances in additive manufacturing of active mechanical metamaterials, Curr. Opin. Solid State Mater. Sci. 24 (2020), 100869, https://doi.org/10.1016/j.cossms.2020.100869.
[7] M. Baniasadi, E. Yarali, M. Bodaghi, A. Zolfagharian, M. Baghani, Constitutive modeling of multi-stimuli-responsive shape memory polymers with multi-functional capabilities, Int. J. Mech. Sci. 192 (2021), 106082, https://doi.org/10.1016/j.ijmecsci.2020.106082.
[8] D.J. Roach, C.M. Hamel, C.K. Dunn, M.V. Johnson, X. Kuang, H.J. Qi, The m4 3D printer: a multi-material multi- method additive manufacturing platform for future 3D printed structures, Addit. Manuf. 29 (2019), 100819, https://doi.org/10.1016/j.addma.2019.100819.
[9] D. Roy, J.N. Cambre, B.S. Sumerlin, Future perspectives and recent advances in stimuli-responsive materials, Prog. Polym. Sci. 35 (2010) 278–301, https://doi.org/10.1016/j.progpolymsci.2009.10.008.
[10] A. Kafle, E. Luis, R. Silwal, H.M. Pan, P.L. Shrestha, A.K. Bastola, 3D/4D printing of polymers: fused deposition modeling (FDM), selective laser sintering (SLS), and stereolithography (SLA), Polymers 13 (2021) 3101, https://doi.org/10.3390/polym13183101.
[11] A.B. Baker, D.F. Wass, R.S. Trask, 4D sequential actuation: combining ionoprinting and redox chemistry in hydrogels, Smart Mater. Struct. 25 (2016) 10LT02, https://doi.org/10.1088/0964-1726/25/10/10LT02.
[12] P. Boyraz, G. Runge, A. Raatz, An overview of novel actuators for soft robotics, Actuators 7 (2018) 48, https://doi.org/10.3390/act7030048.
[13] G. Scalet, Two-way and multiple-way shape memory polymers for soft robotics: an overview, Actuators 9 (2020) 10, https://doi.org/10.3390/act9010010.
[14] N. An, M. Li, J. Zhou, Modeling SMA-enabled soft deployable structures for kirigami/origami reflectors, Int. J. Mech. Sci. 180 (2020), 105753, https://doi.org/10.1016/j.ijmecsci.2020.105753.
[15] Y.L. Yap, S.L. Sing, W.Y. Yeong, A review of 3D printing processes and materials for soft robotics, Rapid Prototyp. J. 26 (2020) 1345–1361, https://doi.org/10.1108/RPJ-11-2019-0302.
[16] G. Decroly, A. Toncheva, L. Blanc, J.M. Raquez, T. Lessinnes, A. Delchambre, P. Lambert, Programmable stimuli-responsive actuators for complex motions in soft robotics: concept, design and challenges, Actuators 9 (2020) 131, https://doi.org/10.3390/act9040131.
[17] J. Mohd, A. Haleem, 4D printing applications in medical field: a brief review, Clin. Epidemiol. Glob. Health 7 (2019) 317–321, https://doi.org/10.1016/j.cegh.2018.09.007.
[18] M.Y. Shie, Y.F. Shen, S.D. Astuti, A.K.X. Lee, S.H. Lin, N.L.B. Dwijaksara, Y. W. Chen, Review of polymeric materials in 4D printing biomedical applications, Polymers 11 (2019) 1864, https://doi.org/10.3390/polym11111864.
[19] A. Mitchell, U. Lafont, M. Hołyńska, C. Semprimoschnig, Additive manufacturing - a review of 4D printing and future applications, Addit. Manuf. 24 (2018) 606–626, https://doi.org/10.1016/j.addma.2018.10.038.
[20] C.M. Hamel, D.J. Roach, K.N. Long, F. Demoly, M.L. Dunn, H.J. Qi, Machine-learning based design of active composite structures for 4D printing, Smart Mater. Struct. 28 (2019), 065005, https://doi.org/10.1088/1361-665X/ab1439.
[21] G. Sossou, F. Demoly, H. Belkebir, H.J. Qi, S. Gomes, G. Montavon, Design for 4D printing: modeling and computation of smart materials distributions, Mater. Des. 181 (2019), 108074, https://doi.org/10.1016/j.matdes.2019.108074.
[22] X. Sun, L. Yue, L. Yu, H. Shao, X. Peng, K. Zhou, F. Demoly, R. Zhao, H.J. Qi, Machine learning-evolutionary algorithm enabled design for 4D-printed active composite structures, Adv. Funct. Mater. 32 (2022) 2109805, https://doi.org/10.1002/adfm.202109805.
[23] F. Demoly, J.C. André, 4D printing: Promises or operational future?, Techniques de l'Ingénieur (2021) RE285, https://doi.org/10.51257/a-v1-re285.
[24] J. Hiller, H. Lipson, Design and analysis of digital materials for physical 3D voxel printing, Rapid Prototyp. J. 15 (2009) 137–149, https://doi.org/10.1108/13552540910943441.
[25] E.L. Doubrovski, E.Y. Tsai, D. Dikovsky, J.M. Geraedts, H. Herr, N. Oxman, Voxel-based fabrication through material property mapping: a design method for bitmap printing, Comput. -Aided Des. 60 (2015) 3–13, https://doi.org/10.1016/j.cad.2014.05.010.
[26] G. Sossou, F. Demoly, H. Belkebir, H.J. Qi, S. Gomes, G. Montavon, Design for 4D printing: a voxel-based modeling and simulation of smart materials, Mater. Des. 175 (2019), 107798, https://doi.org/10.1016/j.matdes.2019.107798.
[27] G. Sossou, F. Demoly, H.J. Qi, S. Gomes, G. Montavon, An additive manufacturing oriented design approach to mechanical assemblies, J. Comput. Des. Eng. 5 (2018) 3–18, https://doi.org/10.1016/j.jcde.2017.11.005.
[28] N. Oxman, Structuring materiality: design fabrication of heterogeneous materials, Archit. Des. 80 (2010) 78–85, https://doi.org/10.1002/ad.1110.
[29] Q. Ge, C.K. Dunn, H.J. Qi, M.L. Dunn, Active origami by 4D printing, Smart Mater. Struct. 23 (2014), 094007, https://doi.org/10.1088/0964-1726/23/9/094007.
[30] Q. Ge, A.H. Sakhaei, H. Lee, C.K. Dunn, N. Fang, M.L. Dunn, Multimaterial 4D printing with tailorable shape memory polymers, Sci. Rep. 6 (2016) 31110, https://doi.org/10.1038/srep31110.
[31] S.T. Ly, J.Y. Ki, 4D printing – fused deposition modeling printing with thermal-responsive shape memory polymers, Int. J. Precis. Eng. Manuf. - Green. Technol. 4 (2017) 267–272, https://doi.org/10.1007/s40684-017-0032-z.
[32] M. Rafiee, R.D. Farahani, D. Therriault, Multi-material 3D and 4D printing: a survey, Adv. Sci. 7 (2020) 1902307, https://doi.org/10.1002/advs.201902307.
[33] D. Roach, Developing intelligent structures and devices using smart materials and multi-material multi-method (M 4) 3D printing. PhD Dissertation, Georgia Institute of Technology, 2021.
[34] Y. Zhang, D. Balkcom. Interlocking structure assembly with voxels. IEEE/RSJ International Conference on Intelligent Robots and Systems, October 9–14, 2016, Daejeon, Korea, 2173–2180.
[35] A. Alsheghri, A. Alageel, O.A. Mezour, M. Sun, B. Yue, S. Tamimi, F. Song, Bio-inspired and optimized interlocking features for strengthening metal/polymer interfaces in additively manufactured prostheses, Acta Biomater. 80 (2018) 425–434, https://doi.org/10.1016/j.actbio.2018.09.029.
[36] C. Shaokang, Z. Lu, Z. Yang, Effect of interlocking structure on mechanical properties of bio-inspired nacreous composites, Compos. Struct. 226 (2019), 111260, https://doi.org/10.1016/j.compstruct.2019.111260.
[37] Z. Yuming, Y. Haimin, C. Ortiz, J. Xu, M. Dao, Bio-inspired interfacial strengthening strategy through geometrically interlocking designs, J. Mech. Behav. Biomed. Mater. 15 (2012) 70–77, https://doi.org/10.1016/j.jmbbm.2012.07.006.
[38] L. Luo, I. Baran, S. Rusinkiewicz, W. Matusik, Chopper: partitioning models into 3D-printable parts, ACM Trans. Graph 31 (2012) 1–9, https://doi.org/10.1145/2366145.2366148.
[39] Q. Zhang, X. Liu, L. Duan, G. Gao, Ultra-stretchable wearable strain sensors based on skin-inspired adhesive, tough and conductive hydrogels, Chem. Eng. J. 365 (2019) 10–19, https://doi.org/10.1016/j.cej.2019.02.014.
[40] S.A. Morin, Y. Shevchenko, J. Lessing, S.W. Kwok, R.F. Shepherd, A.A. Stokes, G. M. Whitesides, Using 'click-e-bricks' to make 3D elastomeric structures, Adv. Mater. 26 (2014) 5991–5999, https://doi.org/10.1002/adma.201401642.
[41] L.J. Young, J. Eom, W.Y. Choi, K.J. Cho, Soft LEGO: Bottom-up design platform for soft robotics, IEEE International Conference on Intelligent Robots and Systems (2018): 7513–7520, https://doi.org/10.1109/IROS.2018.8593546.
[42] L.J. Young, W.B. Kim, J. Eom, W.Y. Choi, K.J. Cho, Soft robotic blocks: Introducing SoBL, a fast-build modularized design block, IEEE Robot. Autom. Mag. 23 (2016) 30–41, https://doi.org/10.1109/MRA.2016.2580479.
[43] X. Yang, S. Druga, Legoons: Inflatable construction kit for children, annual symposium on computer-human interaction in play (2019), 139–146, https://doi.org/10.1145/3341215.3356980.
[44] M. Zhu, F. Zhang, X. Chen, Bioinspired mechanically interlocking structures, Small Struct. 1 (2020) 2000045, https://doi.org/10.1002/sstr.202000045.
[45] X. Jiang, X. Cheng, Q. Peng, L. Liang, N. Dai, M. Wei, C. Cheng, Models partition for 3D printing objects using skeleton, Rapid Prototyp. J. 23 (2017) 54–64, https://doi.org/10.1108/RPJ-07-2015-0091.
[46] M. Yao, Z. Chen, L. Luo, R. Wang, H. Wang, Level-set-based partitioning and packing optimization of a printable model, ACM Trans. Graph. 34 (2015) 1–11, https://doi.org/10.1145/2816795.2818064.
[47] P. Song, B. Deng, Z. Wang, Z. Dong, W. Li, C.W. Fu, L. Liu, CofiFab: coarse-to-fine fabrication of large 3D objects, ACM Trans. Graph. 35 (2016) 1–11, https://doi.org/10.1145/2897824.2925876.
[48] A.K. Jadoon, C. Wu, Y.J. Liu, Y. He, C.C.L. Wang, Interactive partitioning of 3D models into printable parts, IEEE omputer Graph. Appl. 38 (2018) 38–53, https://doi.org/10.1109/MCG.2018.042731658.
[49] A. Deka, S. Behdad, Part separation technique for assembly-based design in additive manufacturing using genetic algorithm, Procedia Manuf. 34 (2019) 764–771, https://doi.org/10.1016/j.promfg.2019.06.208.
[50] Y. Oh, Part decomposition and evaluation based on standard design guidelines for additive manufacturability and assemblability, Addit. Manuf. 37 (2021), 101702, https://doi.org/10.1016/j.addma.2020.101702.
[51] S.J. Luo, Y. Yue, C.K. Huang, Y.H. Chung, S. Imai, T. Nishita, B.Y. Chen, Legolization: optimizing LEGO designs, ACM Trans. Graph. 34 (2015) 1–12, https://doi.org/10.1145/2816795.2818091.
[52] Z. Wang, P. Song, M. Pauly, State of the art on computational design of assemblies with rigid Parts, Comput. Graph. Forum 40 (2021) 633–657, https://doi.org/10.1111/cgf.142660.
[53] S.G. Shih, The art and mathematics of self-interlocking SL blocks, Bridges Conference Proceedings, Tesselations Publishing (2018) 107–114.
[54] D. Qi, N. Milef, S. De, Divided voxels: an efficient algorithm for interactive cutting of deformable objects, Vis. Comput. 37 (2021) 1113–1127, https://doi.org/10.1007/s00371-020-01856-y.
[55] P. Song, C.W. Fu, D. Cohen-Or, Recursive interlocking puzzles, ACM Trans. Graph. 31 (2012) 1–10, https://doi.org/10.1145/2366145.2366147.
[56] Z. Wang, P. Song, M. Pauly, Desia: a general framework for designing interlocking assemblies, ACM Trans. Graph. 37 (2018) 1–14, https://doi.org/10.1145/3272127.3275034.
[57] S. Tibbits, 4D printing: multi-material shape change, Archit. Des. 84 (2014) 116–121, https://doi.org/10.1002/ad.1710.
[58] Q. Ge, H.J. Qi, M.L. Dunn, Active materials by four dimensions printing, Appl. Phys. Lett. 103 (2013), 131901, https://doi.org/10.1063/1.4819837.
[59] P. Rastogi, K. Balasubramanian, Breakthrough in the printing tactics for stimuli-responsive materials: 4D printing, Chem. Eng. J. 366 (2019) 264–304, https://doi.org/10.1016/j.cej.2019.02.085.
[60] A. Costa, A. Abdel-Rahman, B. Jenett, N. Gershenfeld, I. Kostitsyna, K. Cheung Algorithmic approaches to reconfigurable assembly systems, IEEE Aerospace Conference (2019), 2–9 March, Big Sky, MT, USA, https://doi.org/10.1109/AERO.2019.8741572.
[61] H. Medellín, T. Lim, J. Corney, J.M. Ritchie, J.B.C. Davies, Rapid prototyping through octree decomposition of 3D geometric models, ASME Design Engineering Technical Conference (2004) 843–852, https://doi.org/10.1115/DETC2004–57769.

[62] M. Delmans, J. Haseloff, μCube: a framework for 3D printable optomechanics, J. Open Hardw. 2 (2018), https://doi.org/10.5334/joh.8.
[63] D. Wang, M. Hermes, R. Kotni, Y. Wu, N. Tasios, Y. Liu, B. de Nijs, E.B. van der Wee, C.B. Murray, M. Dijkstra, A. van Blaaderen, Interplay between spherical confinement and particle shape on the self-assembly of rounded cubes, Nat. Commun. 9 (2018) 2228, https://doi.org/10.1038/s41467-018-04644-4.
[64] L. Aaron, N. Michelson, B. Minevich, Y. Fleger, M. Stern, A. Shaulov, Y. Yeshurun, O. Gang, DNA-assembled superconducting 3D nanoscale architectures, Nat. Commun. 11 (2020) 5697, https://doi.org/10.1038/s41467-020-19439-9.
[65] L. Yuan, S. Zhuo, Y. Xiao, G. Zheng, G. Dong, F.Z. Yaoyao, Rapid modeling and design optimization of multi-topology lattice structure based on unit-cell library, J. Mech. Des. 142 (2020), 091705, https://doi.org/10.1115/1.4046812.
[66] B. Jenett, N. Gershenfeld, M. Carney, S. Calisch, W. Spencer, Digital morphing wing: active wing shaping concept using composite lattice-based cellular structures, Soft Robot. 4 (2017) 33–48, https://doi.org/10.1089/soro.2016.0032.
[67] J. Zhu, H. Zhou, C. Wang, L. Zhou, S. Yuan, W. Zhang, A review of topology optimization for additive manufacturing: status and challenges, Chin. J. Aeronaut. 34 (2021) 91–110, https://doi.org/10.1016/j.cja.2020.09.020.
[68] A. Ion, L. Wall, R. Kovacs, P. Baudisch, Digital mechanical metamaterials, Conference on Human Factors in Computing Systems (2017) 977–88, https://doi.org/10.1145/3025453.3025624.
[69] V. Hahn, P. Kiefer, T. Frenzel, J. Qu, E. Blasco, C. Barner-Kowollik, M. Wegener, Rapid assembly of small materials building blocks (voxels) into large functional 3D metamaterials, Adv. Funct. Mater. 30 (2020) 1907795, https://doi.org/10.1002/adfm.201907795.
[70] P. Song, Z. Fu, L. Liu, C.W. Fu, Printing 3D objects with interlocking parts, Comput. Aided Geom. Des. 35-36 (2015) 137–148, https://doi.org/10.1016/j.cagd.2015.03.020.
[71] F. Demoly, X.T. Yan, B. Eynard, L. Rivest, S. Gomes, An assembly oriented design framework for product structure engineering and assembly sequence planning, Robot. Comput. Integr. Manuf. 27 (2011) 33–46, https://doi.org/10.1016/j.rcim.2010.05.010.
[72] K. Tang, P. Song, X. Wang, B. Deng, C.W. Fu, L. Liu, Computational design of steady 3D dissection puzzles, Comput. Graph. Forum 38 (2019) 291–303, https://doi.org/10.1111/cgf.13638.
[73] J. Lai, X. Ye, J. Liu, C. Wang, J. Li, X. Wang, M. Ma, M. Wang, 4D printing of highly printable and shape morphing hydrogels composed of alginate and methylcellulose, Mater. Des. 205 (2021), 109699, https://doi.org/10.1016/j.matdes.2021.109699.